

Measurement of $b \rightarrow u\ell\nu_\ell$ at Belle II

Andrea Fodor ^{†*}

*McGill University,
845 Sherbrooke Street West, Montreal, Canada*

E-mail: afodor@physics.mcgill.ca

The semileptonic B meson decays of the type $B \rightarrow X_u\ell\nu$ are important for measuring the V_{ub} CKM matrix element. Recent measurements of inclusive $B \rightarrow X_u e\nu_e$ and hadronic-tagged $B^0 \rightarrow \pi^-\ell^+\nu$ from the Belle II experiment are presented. The results are obtained using the data collected at Belle II between March 2019 and March 2020, with the total luminosity of 37.8 fb^{-1} . These preliminary measurements are used to validate the detector and reconstruction software performance. The measured preliminary branching fraction of $B^0 \rightarrow \pi^-\ell^+\nu$, equal to $(1.58 \pm 0.43_{\text{stat}} \pm 0.07_{\text{sys}}) \cdot 10^{-4}$, is in agreement with the world average.

*BEAUTY2020
21-24 September 2020
Kashiwa, Japan (online)*

[†]On behalf of the Belle II Collaboration.

*Speaker

1. Introduction

The Belle II experiment is a B -factory experiment located at the KEK laboratory in Tsukuba, Japan. The SuperKEKB accelerator collides electrons and positrons at the center of mass (COM) energy of 10.58 GeV¹ at the interaction point inside the Belle II detector. At this center of mass energy the $\Upsilon(4S)$ is copiously produced. $\Upsilon(4S)$ decays almost exclusively to B meson pairs, B^+B^- or $B^0\bar{B}^0$. Belle II started operating in March 2019. The results presented here use the data collected between March 2019 and March 2020, corresponding to 37.8 fb⁻¹, of which 34.6 fb⁻¹ was taken at COM energy of 10.58 GeV, corresponding to the $\Upsilon(4S)$ resonance, and 3.2 fb⁻¹ was taken 60 MeV below $\Upsilon(4S)$ resonance.

The Belle II detector consists of the vertex detector (VXD), the central drift chamber (CDC), time of propagation counter and proximity focusing aerogel ring imaging Cherenkov detector used for particle identification (PID), the electromagnetic calorimeter (ECL), and the K_L and muon detector (KLM). The sub-detectors are described in detail in Ref. [1].

One of the goals at the core of the Belle II physics program is the precision measurement of Cabibbo-Kobayashi-Maskawa (CKM) matrix elements. Semileptonic decays of B mesons play a critical role in the determination of the magnitudes of the CKM quark-mixing matrix elements $|V_{cb}|$ and $|V_{ub}|$. The decays of the type $b \rightarrow u\ell\nu$ are important for measuring the CKM matrix element $|V_{ub}|$. This is a challenging measurement due to the presence of a neutrino in the final state, which cannot be detected and manifests as missing energy in the event. This decay is suppressed compared to the decay with the charm quark in the final state, $b \rightarrow c\ell\nu$, which is the main background for this mode. Depending on the treatment of the final state meson, two different analysis approaches exist. Exclusive analysis approaches involve explicit reconstruction of the charmless meson. Inclusive analysis approaches only select the final state charged lepton, without explicitly reconstructing the final state meson. Previous results show tension between inclusive and exclusive measurements of the $|V_{ub}|$ matrix element [2]. Figure 1 summarizes previous results of inclusive and exclusive $|V_{ub}|$ measurements.

Here we will present the searches for the untagged $B \rightarrow X_u e \nu_e$ decay and the $B^0 \rightarrow \pi^- \ell^+ \nu_\ell$ by Belle II. While the results are not yet competitive with the current world averages, they demonstrate the performance of the Belle II detector and the analysis software, and pave the way for more precise searches in the future with larger datasets.

2. Untagged inclusive $B \rightarrow X_u e \nu_e$

We performed a search for $B \rightarrow X_u \ell \nu_\ell$ decays. This was done inclusively, where only the outgoing lepton was selected. The accompanying hadron and the neutrino were not reconstructed. Untagged analysis approach was used, where the companion B meson is not reconstructed. The lepton momentum endpoint was examined, to avoid the dominant background from the decay $B \rightarrow X_c \ell \nu_\ell$. Since the u quark is lighter than c quark, the electron from $B \rightarrow X_u \ell \nu$ decay has more energy available, and thus can have higher momentum, with electrons from $B \rightarrow X_c \ell \nu$ reaching a maximum momentum of about 2.4 GeV, and electrons from $B \rightarrow X_u \ell \nu$ reaching 2.8 GeV in the COM frame.

¹Natural units, with $c = 1$ are used throughout this report.

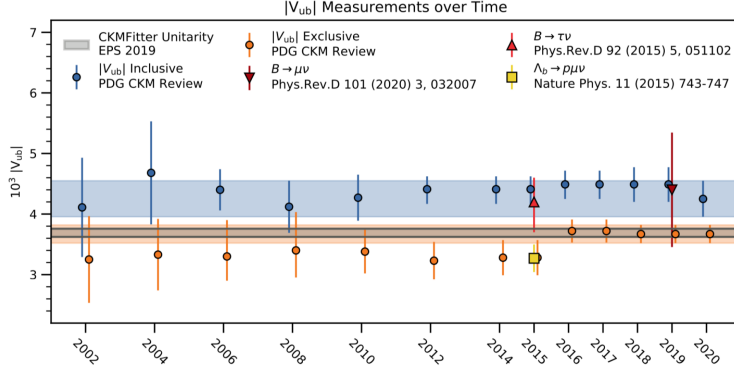


Figure 1: Measurements of $|V_{ub}|$ over time; the blue points show the results of inclusive $|V_{ub}|$ measurements [2], while the orange points show the results of exclusive measurements [2]. The blue and orange bands show the combined uncertainty of inclusive and exclusive measurements, respectively. The red triangles show the results of purely leptonic searches, $B \rightarrow \tau\nu$ [3](red triangle) and $B \rightarrow \mu\nu$ [4](red upside down triangle). The yellow square shows the result from $\Lambda_b \rightarrow p\mu\nu$ [5]. The grey band shows the average obtained by the CKMfitter group [6][7].

The signal electron was identified using particle identification (PID) algorithms. Multivariate training using event shape variables was performed to suppress the continuum backgrounds, where $e^+e^- \rightarrow u\bar{u}, d\bar{d}, s\bar{s}, c\bar{c}, \ell\bar{\ell}$. The most important variable in the training was the Fox-Wolfram R2 moment [1]. The signal yield was extracted from the electron momentum in the COM frame in the endpoint region, [2.1, 2.8] GeV. Comparison between data and Monte Carlo (MC) of the electron spectrum endpoint is shown in Fig. 2(a).

Fit was performed on the electron spectrum to estimate the remaining continuum contributions. Off-resonance data, taken 60 MeV below the $\Upsilon(4S)$ resonance, was used to estimate the continuum contributions. The fit was performed on off-resonance data in the momentum range [1.0, 3.3] GeV, and simultaneously on on-resonance data in the region above 2.8 GeV, where the contributions from B meson decays are not significant. Binned (50 MeV) chi-squared minimization was used, with the function describing the electron spectrum:

$$f(p_i) = a_0 \cdot \exp(a_1 p_i + a_2 p_i^2 + a_3 p_i^3) + \exp(a_4 p_i + a_5 p_i^2),$$

where p_i is the COM electron momentum in the i -th bin, a_0, \dots, a_5 are the fit parameters. The electron spectrum in the off-resonance and on-resonance data is shown in Fig. 2(b).

The backgrounds from $B\bar{B}$ decays, such as $B \rightarrow X_c \ell \nu$, secondary electrons not originating from B meson decays, electrons from J/ψ decays, and other, were estimated using a MC template fit. Binned chi-square minimization was performed in the range [1.0, 3.3] GeV in bins of 50 MeV, with the continuum backgrounds described with off-resonance fit. Continuum and background $B\bar{B}$ contributions obtained from the fits were then subtracted from the measured data in the endpoint region of the electron momentum, between 2.1 and 2.8 GeV, as shown in Fig. 3. The observed excess is consistent with $B \rightarrow X_u e \nu_e$ prediction at 3σ .

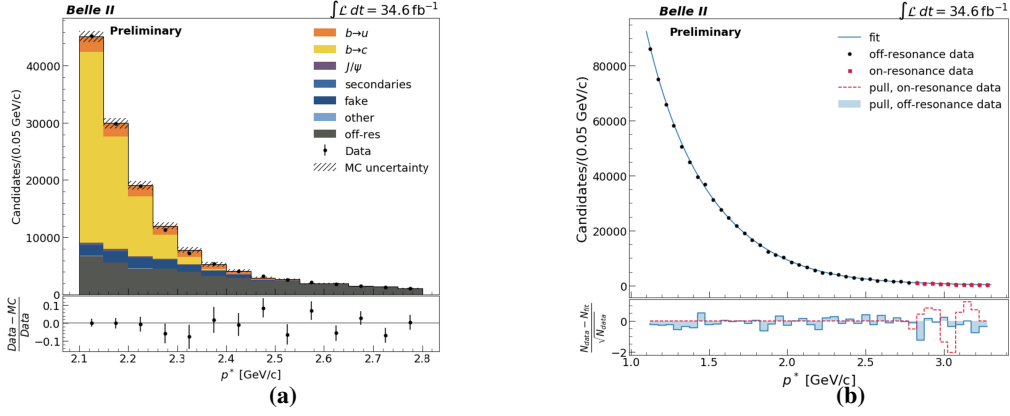


Figure 2: Left: comparison of data and MC electron COM momentum spectrum in the endpoint region; $b \rightarrow u$ and $b \rightarrow c$ represent all $B \rightarrow X_u\ell\nu$ and $B \rightarrow X_c\ell\nu$ events that pass the selection, respectively; J/ψ represents the electrons that originate from $J/\psi \rightarrow e^+e^-$ decays; secondaries represent electrons that are not originating from a B meson or J/ψ decay; fakes represent other particles misidentified as electrons. Right: electron spectrum in the off-resonance sample (black points) and in the on-resonance sample (red squares); the fit used to estimate the continuum contributions is shown with the blue line; the measure of goodness of fit is shown in the lower panel.

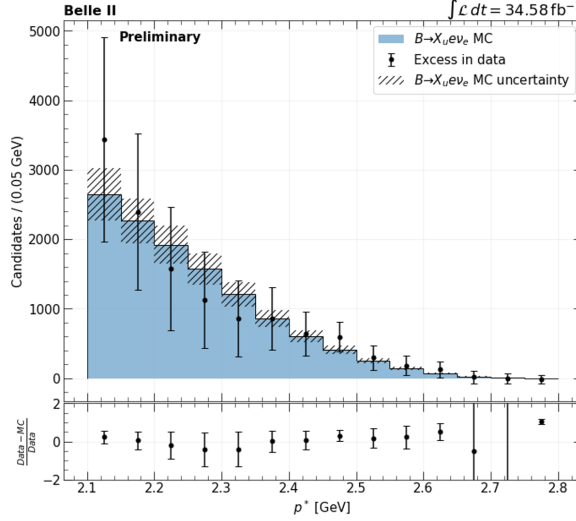


Figure 3: Comparison between $B \rightarrow X_u\ell\nu_e$ MC and the excess events in data in the electron endpoint region after the continuum and $B\bar{B}$ backgrounds subtraction.

3. Tagged exclusive $B^0 \rightarrow \pi^-\ell^+\nu_\ell$

A search for the decay² $B^0 \rightarrow \pi^-\ell^+\nu_\ell$ [8], where $\ell = e, \mu$, was performed using hadronic tagging provided by the Full Event Interpretation (FEI) algorithm [9]. The FEI algorithm is a tagging algorithm developed at Belle II that uses machine learning for decay reconstruction. In FEI, one of the two B mesons produced in the event is reconstructed exclusively in one of the 4000 available hadronic or semileptonic decay modes. A multivariate algorithm is used with a hierarchical

²Charge conjugation is implied throughout this report.

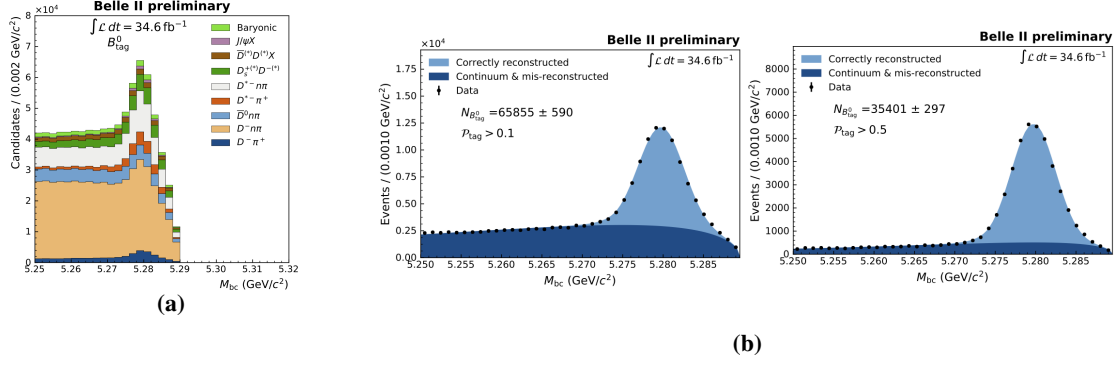


Figure 4: (a): FEI reconstructed $B_{\text{tag}}^0 M_{bc}$ for different hadronic B^0 reconstruction channels; (b): FEI reconstructed $B_{\text{tag}}^0 M_{bc}$ for different cuts on \mathcal{P}_{tag} . Equivalent plots for B_{tag}^+ can be found in Ref. [10]

approach: first the detected tracks, clusters and vertices are used as final state particle candidates; these final state candidates are then combined to reconstruct intermediate state candidates; finally, all the candidates are combined to reconstruct the B meson candidates, B_{tag} . The assigned classifier value, \mathcal{P}_{tag} , between 0 and 1, discriminates poorly reconstructed or misreconstructed from correctly reconstructed B_{tag} candidates. The FEI outputs multiple B_{tag} candidates per event, which can be further reduced by setting requirements on beam-constrained mass, M_{bc} , and energy difference w.r.t. the e^+e^- system energy in the COM frame:

$$M_{bc} = \sqrt{\frac{E_{\text{beam}}^2}{4} - \vec{p}_{B_{\text{tag}}}^2}, \quad \Delta E = E_{B_{\text{tag}}} - \frac{E_{\text{beam}}}{2},$$

where $\vec{p}_{B_{\text{tag}}}$ and $E_{B_{\text{tag}}}$ are the FEI reconstructed B_{tag} momentum and energy in the COM frame. During the hadronic FEI reconstruction, the requirements are $M_{bc} > 5.24$ GeV and $|\Delta E| < 0.2$ GeV. The distribution of $B_{\text{tag}}^0 M_{bc}$ for different hadronic B^0 reconstruction channels is shown in Fig. 4(a), and in Fig. 4(b) for different cuts on \mathcal{P}_{tag} .

By exclusively reconstructing one B meson using hadronic modes, one can infer the momentum and direction of signal B candidate:

$$p_{\text{sig}} \equiv (E_{B_{\text{sig}}}, \vec{p}_{B_{\text{sig}}}) = \left(\frac{m(\Upsilon(4S))}{2}, -\vec{p}_{B_{\text{tag}}} \right).$$

The ability to infer the four-momentum of the signal B candidate makes this approach well suited for signal decays with neutrinos which contain missing energy signatures.

In the $B^0 \rightarrow \pi^- \ell^+ \nu_\ell$ analysis FEI hadronic tagging was used to identify B_{tag} candidates. Loose cut on FEI classifier output, $\mathcal{P}_{\text{tag}} > 0.001$, was used to minimize the signal loss. The requirement on B_{tag} beam-constrained mass was tightened to avoid miss-reconstructed candidates, with $M_{bc} > 5.27$ GeV. A muon or electron candidate, and an oppositely charged pion candidate were identified using PID algorithms from the remaining detector signal not associated with the B_{tag} . The continuum type backgrounds were suppressed using a cut on Fox-Wolfram R2 moment, $R2 < 0.4$. Signal yield was extracted using the distribution of the square of the missing mass:

$$M_{\text{miss}}^2 \equiv p_{\text{miss}}^2,$$

$$p_{miss} \equiv (E_{miss}, \vec{p}_{miss}) = p_{B_{sig}} - p_Y,$$

where p_Y is the combined momentum of the pion and the charged lepton. One $\Upsilon(4S)$ candidate with the lowest M_{miss}^2 value was retained per event. The analysis was performed blinded in the signal region $M_{miss}^2 < 1 \text{ GeV}^2$. Fits were performed on the M_{miss}^2 distribution to obtain the signal yields. Template Probability Density Functions (PDFs) were constructed from signal and background M_{miss}^2 distributions in MC. An extended unbinned maximum likelihood fit was performed on M_{miss}^2 distribution in data using the template MC PDFs. Pre-fit and fitted M_{miss}^2 distributions are shown in Fig. 5. The resulting signal yield from the fit is 20.79 ± 5.68 , which is in good agreement with the predicted value from signal MC of 19.83. The observed significance is 5.69σ .

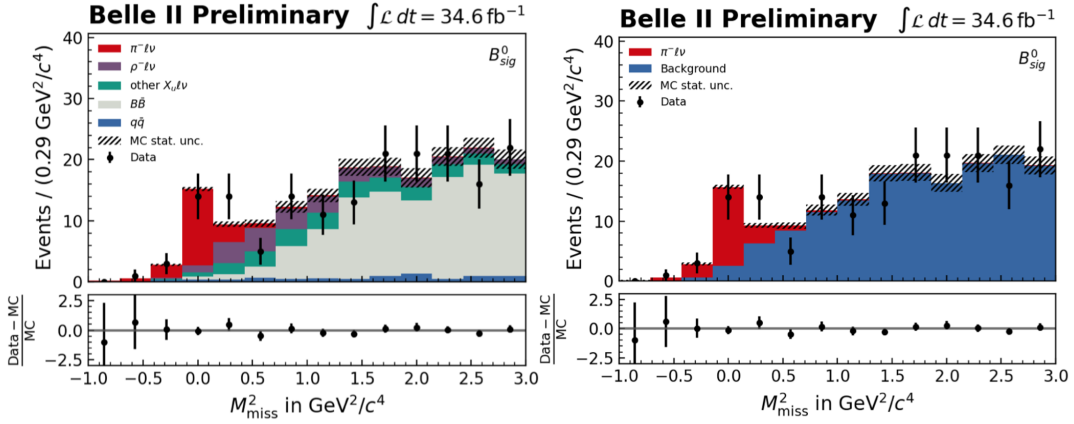


Figure 5: Pre-fit (left) and fitted (right) M_{miss}^2 distributions.

The $B^0 \rightarrow \pi^- \ell^+ \nu_\ell$ branching fraction was calculated using the following formula:

$$\mathcal{B}(B^0 \rightarrow \pi^- \ell^+ \nu_\ell) = \frac{N_{sig}^{data}(1 + f_{+0})}{4 \cdot C_{FEI} \cdot N_{B\bar{B}} \cdot \epsilon},$$

where N_{sig}^{data} is the fitted signal yield obtained from data, f_{+0} is the ratio between the branching fractions of the decays of the $\Upsilon(4S)$ meson to pairs of charged and neutral B mesons [2], C_{FEI} is the FEI calibration factor, $N_{B\bar{B}}$ is the number of B meson pairs counted in the dataset used, and ϵ is the reconstruction efficiency. The FEI calibration factor was obtained by comparing the efficiency of FEI in data and MC using inclusive $B \rightarrow X\ell\nu$ events. It is equal to 0.83 ± 0.03 [10]. The signal efficiency determined from signal MC is $(0.216 \pm 0.001)\%$. The resulting branching fraction is $\mathcal{B} = (1.58 \pm 0.43_{stat} \pm 0.07_{sys}) \cdot 10^{-4}$. The result is in agreement with the world average value, $(1.50 \pm 0.06) \cdot 10^{-4}$ [2]. The evaluation of systematic uncertainties is described in Ref. [8].

4. Summary and prospects for $b \rightarrow u$ measurements at Belle II

We presented here the preliminary measurements of $B \rightarrow X_u e \nu_e$ and $B^0 \rightarrow \pi^- \ell^+ \nu$ semileptonic B -meson decay modes. The preliminary measured $B^0 \rightarrow \pi^- \ell^+ \nu$ branching fraction of $(1.58 \pm 0.43_{stat} \pm 0.07_{sys}) \cdot 10^{-4}$ is in agreement with previous results. Significant improvement on these and other $b \rightarrow u$ semileptonic measurements is expected with higher luminosities and better

understanding of the detector performance. Overall, the $|V_{ub}|$ precision will be improved to 3% with the full 50 ab^{-1} dataset at Belle II. With improved theoretical uncertainties available, $B \rightarrow \pi\ell\nu$ is expected to be the golden mode for $|V_{ub}|$ measurement.

References

- [1] Kou, E., *et al.* (Belle II collaboration) "The Belle II Physics Book." PTEP 2019 (2019) no. 12, 123C01.
- [2] Tanabashi, M., *et al.* (Particle Data Group), Phys. Rev. D **98**, 030001 (2018) and 2019 update.
- [3] Kronenbitter, B., *et al.* (Belle collaboration) "Measurement of the branching fraction of $B^+ \rightarrow \tau\nu_\tau$ decays with the semileptonic tagging method." Phys. Rev. D 92, 051102 (2015).
- [4] Prim, M., *et al.* "Search for $B^+ \rightarrow \mu^+\nu_\mu$ and $B^+\mu^+N$ with inclusive tagging." Phys. Rev. D 101, 032007 (2020).
- [5] Aaij, R., *et al.* (LHCb collaboration) "Determination of the quark coupling strength $|V_{ub}|$ using baryonic decays." Nature Phys 11, 743-747 (2015).
- [6] CKMfitter Group, EPS 2019 conference
- [7] Prim, M., plot obtained in private correspondence
- [8] Abudinen, F., *et al.* (Belle II collaboration) "Exclusive $B^0 \rightarrow \pi^-\ell^+\nu_\ell$ Decays with Hadronic Full Event Interpretation Tagging in 34.6 fb^{-1} of Belle II Data." arXiv preprint arXiv:2008.08819 (2020).
- [9] Keck, T., *et al.* "Full Event Interpretation – An exclusive tagging algorithm for the Belle II experiment." Comput Softw Big Sci (2019) 3: 6.
- [10] Abudinen, F., *et al.* (Belle II collaboration) "A calibration of the Belle II hadronic tag-side reconstruction algorithm with $B \rightarrow X\ell\nu$ decays." arXiv preprint arXiv:2008.06096 (2020).